The Micelle-Associated 3D Structures of Boc-Y(SO_3)-Nle-G-W-Nle-D-2-phenylethylester (JMV-180) and CCK-8(s) Share Conformational Elements of a Calculated CCK_1 Receptor-Bound Model

Mohanraja Kumar,[†] Joseph R. Reeve, Jr.,*[,†] Weidong Hu,[‡] Laurence J. Miller,[§] and David A. Keire[†]

CURE: Digestive Diseases Research Center, VA Greater Los Angeles Healthcare System, Los Angeles, California 90073 Digestive Diseases Division, UCLA School of Medicine, Los Angeles, California 90095, Division of Immunology, Beckman Research Institute of the City of Hope, Duarte, California 90010, Department of Molecular Pharmacology and Experimental Therapeutics, Mayo Clinic, Scottsdale, Arizona 85259

Received November 7, 2007

JMV-180 (**1**) and CCK-8(s) are high affinity ligands at the CCK_1 receptor that have similar and different actions via this receptor. Here we calculate the tertiary structure of **1** or CCK-8(s) in the presence of dodecylphosphocholine micelles at pH 5.0 and 35 °C from 2D ^{1}H NMR data recorded at 600 MHz. The NMR derived 3D structures of **1** and CCK-8(s) share a common type I β-turn around residues Nle3/M3 and G4 and diverge from each other structurally at the N- and C-termini. The fluorescence and circular dichroism spectral properties of these peptides are consistent with their NMR derived structures. The structures determined in the presence of DPC micelles are compared to available models of **1** or CCK-8(s) bound to the CCK_1 receptor. For CCK and **1**, these comparisons show that DPC micelle associated structures duplicate some important aspects of the models calculated from cross-linking derived constraints at the CCK_1 receptor.

Cholecystokinin is a gastrointestinal hormone that stimulates pancreatic exocrine secretion, gall bladder contraction, and inhibits gastric motility and food intake.[1] All of these actions are mediated by the CCK_1[a] receptor subtype, which has two different affinity states[2–4] with low (K_d = 2.2 nM) or high (K_d = 13 pM) potency for CCK-8(s) binding.[2] Food intake is moderated by the low affinity state of the receptor,[5] while the other actions are regulated via the high affinity state.[6] Activation of the low affinity state of this receptor by large (micromolar) amounts of CCK-8(s) leads to pancreatitis in intact rodents and to correlative changes in rodent pancreatic acinar cells.[7] In addition, cholecystokinin can also activate CCK_2 receptors that are involved in gastric acid secretion.[8]

JMV-180 (**1**) is a cholecystokinin receptor agonist that has been extensively studied which selectively binds and activates the high affinity state of the CCK_1 receptor in rodents.[4] In addition, **1** is an *antagonist* for the rat and an *agonist* for the mouse at the low affinity state of the CCK_1 receptor. Therefore, **1** acts in different ways via the CCK_1 receptor depending on the tissue, species being studied, or biological event assayed.[6,9–12] These differences in action of **1** at the CCK_1 receptor lead to similar or differing biological activity compared to other CCK_1 agonists such as CCK-8(s) depending on the assay. For example, CCK-8(s) and **1** are different in potency but the same in efficacy for binding of the high affinity state of the CCK_1 receptor, stimulation of cyclic intracellular calcium release, and release of pancreatic enzymes. By contrast to **1**, high doses of CCK-8(s) cause global release of calcium, supramaximal inhibition of pancreatic enzyme release, and acute pancreatitis.[13] Differences in the action of CCK-8(s) and **1** may be the result of differences in the spatial arrangement of the elements of the peptide ligands, which interact with receptor residues to induce conformational change and the concomitant signal transduction into the cell interior. Therefore, interest is high in determining the tertiary structures of these ligands bound to receptors for drug design.

Because of the difficulty in obtaining experimental data for 3D structures of high affinity ligand/receptor complexes, as a first step, the structures of the ligands in solution in the absence of receptor have been used for structure-based drug design. However, the utility of using solution structures for rational design of agonists for the CCK_1 receptor is in question because peptide ligands with 10 or fewer amino acids (i.e., CCK-8 and **1**) tend to be flexible in solution. In aqueous solution, CCK-8(s) has been reported to have some population of interchanging conformations with a central β-turn around G4 and W5 followed by a γ-turn involving the M6-D7-F8 sequence of the peptide (see ref 14 in Table 1). The aqueous solution structure of **1** has not been studied by NMR presumably because of the peptides poor solubility. In the case of flexible solution structures, there is no way to know which conformation from an ensemble of structures is selected by enthalpy and entropy to bind and activate the receptor.

A second approach is to solve the tertiary structure of the receptor−ligand in the presence of lipid micelles with extracellular portions of the receptor present by NMR methods.[15,16] NMR methods are a well established method for probing the structure and dynamics of peptide ligands in the presence of micelles.[17–20] In this model, a peptide may associate with the cell surface lipids by insertion of hydrophobic residues and electrostatic interactions with charged lipid headgroups to form a unique 3D conformation that "prepays" some of the energetic cost of ligand desolvation prior to receptor binding.[21–23] This

* To whom correspondence should be addressed. Phone: 310-268-3935. Fax: 310-268-4963. E-mail: jreeve@ucla.edu. Address: VA GLAHS/CURE, Building 115, Room 120, 11301 Wilshire Boulevard, Los Angeles, CA, 90073.

† CURE: Digestive Diseases Research Center, VA Greater Los Angeles Healthcare System, Digestive Diseases Division, UCLA School of Medicine.

‡ Division of Immunology, Beckman Research Institute of the City of Hope.

§ Department of Molecular Pharmacology and Experimental Therapeutics, Mayo Clinic.

[a] Abbreviations: CD, circular dichroism; NOE, nuclear Overhauser effect; NOESY, nuclear Overhauser effect spectroscopy; TOCSY, total correlation spectroscopy; NATA, *N*-acetyl tryptophan amide; rmsd, root-mean-square-deviation; DPC, dodecylphosphocholine; (Nle) norleucine; CCK-8(s), D-Y(SO_3)-M-G-W-M-D-F-amide; CCK-8(ns), D-Y-M-G-W-M-D-F-amide; CCK_1, cholecystokinin receptor type 1.

10.1021/jm701401j CCC: $40.75
Published on Web 06/10/2008

Table 1. Selected Structure Studies on CCK Analogues

peptide	solution conditions	methods	results	ref
CCK-8 and CCK-7 (ns or s)[a]	DMSO[b]/H_2O	^{1}H NMR, fluorescence	β-turn-G4-W5-M6-D7 γ-turn-M6-D7-F8	14, 79
CCK-8(s)	DMSO	^{1}H NMR and MD study	β- and γ-turn	80
[T^3, Nle^6]CCK-9(s)[c]	DMSO/H_2O/5 °C	2D-NMR, AMBER-SYBYL	γ-turn-centered on T3	81
CCK-8(ns) and CCK-15(ns)	HFA[d]/H_2O	2D-NMR, DYANA	helical	75
CCK-15(s) (Mierke group)	DPC, pH 5.2, 50 mM phosphate	2D-NMR, DG-MD[e]	helical	74
CCK-8(ns) (Mierke group)	DPC, pH 6.5, 298, 308, and 318 K	2D-NMR, DG-MD[e]	helical	16
CCK-8(s) bound to CCK_1 receptor (Fourmy group)	computer model	Accelrys software/AutoDock	helical	34
1 bound to CCK_1 receptor (Fourmy group)	computer model	Accelrys software/AutoDock	helical	34
[$Nle^{3,6}$]CCK-8(s) bound to CCK_1 receptor (Miller group)	computer model	Internal Coordinate Mechanics software package	β-turn around Nle3 and G4	32
CCK-8(s)	DPC, pH 5, 50 mM phosphate, 308 K	2D-NMR, CD, fluorescence, XPLOR	type I β-turn, M3-G4	this work
1	DPC, pH 5, 50 mM phosphate, 308 K	2D-NMR, CD, fluorescence, XPLOR	type I β-turn, Nle3-G4	this work

[a] ns = nonsulfated tyrosine, s = sulfated tyrosine. [b] DMSO = dimethyl sulfoxide. [c] [T^3,Nle^6]CCK-9(s) substitutions denoted using CCK-8 numbering for comparison purposes. [d] HFA = 1,1,1,3,3,3-hexafluoroacetone. [e] DG-MD = distance geometry-molecular dynamics in H_2O−decane cell.

lipid-induced conformation is transported via the bilayer to its receptor-binding pocket located in a transmembrane portion of the receptor. If this model is correct, the lipid-induced tertiary structure of a peptide could be the conformation that initially binds to the receptor. Because of sensitivity limitations, these NMR studies must be performed in the presence of millimolar concentrations of the ligand and the receptor fragment. Mierke's laboratory has shown specific sites of interaction between nonsulfated CCK-8 (a low potency CCK_1 ligand) and an N-terminal or third extracellular loop portion of the CCK_1 receptor. In addition, this group has reported that the CCK-8(ns) helical structure in the presence of DPC micelles is insensitive to N-terminal extension of the peptide to 15 residues or sulfation of the tyrosine in position 2. Finally these authors show that CCK-8(ns) maintains a helical-like structure in the presence of receptor fragments.[24]

Regrettably, there is little evidence that portions of CCK_1 receptor (i.e., extracellular loops, N- or C-terminal segments) can be reconstituted in micelles with their native conformations intact. Indeed, the question of "What are the native conformations of the receptor loops?" has not been answered for the CCK receptors. Therefore no validating comparison can be made between what is observed by Mierke's group and the actual structure of this loop in the intact receptor. Most current models of GPCRs are based on homology modeling of the X-ray crystal structure of rhodopsin, which may or may not be appropriate for peptide receptors.[25]

Recently, a new crystal structure has been published that may improve the available models: Cherezov et al. reported the crystal structure of the GPCR β_2-adrenergic receptor-T4 lysozyme fusion protein bound to a catecholamine analogue (carazolol) at 2.4 Å resolution.[26,27] These authors show that the rhodopsin receptor and the β_2-adrenergic receptor are different in important aspects of how their nonpeptide ligands bind these receptors. This highlights the importance of having more structures available for comparison in order to differentiate between common features of peptide binding to GPCRs and features unique to a receptor that impart specificity for a given peptide. We note that these static models of peptide−receptor association may lack dynamic components that are important to receptor function.[28]

Ideally, to understand the molecular mechanism of CCK-8(s) biological action, one would determine the structure of the peptide ligand bound to its receptor and the dynamics of the interaction by NMR methods. Unfortunately, for the CCK_1 receptor, current NMR methods have not supplied the necessary spatial information at low angstrom resolution to generate the tertiary structures of the membrane associated receptor or of the native *high affinity* ligand−receptor complex. One NMR study has reported structure of a *low affinity* peptide analogue bound to a lipid-reconstituted G-protein coupled receptor in aqueous solution:[29] Inooka et al. determined the structure of a pituitary-adenylate-cyclase-activating polypeptide analogue (PACAP(1-21)-NH_2) bound to the PACAP receptor. The lipid associated structure of PACAP(1-21)-NH_2 was only altered at the seven N-terminal residues in the presence of the receptor. Their study required the expression of milligram quantities of receptor, solubilization of the receptor in digitonin, development of a ligand with lowered affinity for the receptor, and collection of NMR data on an 800 MHz spectrometer.[29]

In a second NMR study, frozen samples of a high affinity neurotensin (NT) analogue bound to the neurotensin-1 receptor (NTS-1) showed a low resolution extended backbone conformation for NT.[30] These authors purified milligram amounts of NTS-1 receptor from an *Escherichia coli* expression system, reconstituted the receptor in lipid vesicles, synthesized uniformly labeled [^{13}C, ^{15}N]-NT(8−13), and conducted solid state NMR studies on a 600 MHz wide-bore spectrometer at −80 °C. Subsequent studies with [^{13}C, ^{15}N]-NT(8−13) in the presence of only lipid showed little overlap between the receptor bound conformational space of the ligand with that found in a lipid environment.[31] For the NT/NTS-1 case, these data would argue against a lipid mediated receptor association pathway.

In this work, we investigated a third NMR approach that is based on the supposition that the structure of the ligand in a lipid membrane without the receptor present could play a role in CCK_1 receptor binding and activation. This approach is lent credence by the work on PACAP because these authors observed that the lipid micelle bound structure and the receptor-bound structure of their PACAP analogue shared a common helical region.[29] By contrast, this approach is not supported by the solid state NMR data reported for NT.

Fortunately, there are static models for the CCK-8(s)-CCK_1 receptor complex available to test the hypothesis that lipid-associated CCK-8(s) or **1** structures are relevant for binding and activation of the CCK_1 receptor. In these models, molecular modeling is used in conjunction with direct experimental evidence to generate plausible models of the ligand-occupied receptor. For the CCK receptors, two distinct approaches have been taken, and they have yielded quite different molecular

models. In one, the molecular model has been developed predominantly based on photoaffinity labeling, utilizing intrinsic probes with sites of covalent attachment that are distributed throughout the pharmacophoric domain of the ligand.[32] This generates spatial approximation constraints that establish which ligand residues are adjacent to which receptor residues. The contrasting model has been developed based predominantly on mutagenesis data.[33,34] This approach probes the loss of function observed in response to receptor mutagenesis as well as the functional impact of complementary modifications of the receptor and ligand residues that are postulated to interact with each other. Of particular interest, the receptors in these two models are quite similar, particularly in their helical bundle domains, although few experimentally derived constraints have been applied to the loop domains. Interestingly, the amino-terminal regions of CCK-8 are also situated similarly in the two models. The major difference is in the placement of the carboxyl-terminal end of CCK-8. In the photoaffinity labeling-driven model, this is outside the bilayer adjacent to the amino-terminal tail of the receptor. In contrast, in the mutagenesis-driven model, it is placed deep in the intramembranous helical bundle.

For this work, we present data that examines the interaction of two high affinity CCK_1 receptor agonists, CCK-8(s) and **1**, with perdeuterated dodecylphosphocholine micelles and compare and contrast their 3D structures. We then compare our structures to the structure of nonsulfated CCK-8 determined by the Mierke group in the presence of DPC micelles with residues 1−47 of the CCK_1 receptor present (1D6G). In addition, we compare our structures to the models published by the Fourmy or Miller groups that present structures of CCK-8(s) or **1** bound to the CCK_1 receptor. On the basis of these comparisons, we suggest that the use of micelle-associated peptide tertiary structures as models of CCK_1 receptor bound ligands does offer insight into receptor-associated ligand conformations.

Materials and Methods

Both **1** and CCK-8(s) peptides were purchased from Research Plus (Bayonne, NJ) and used as purchased. On the basis of the data supplied by Research Plus, the peptides (**1** and CCK-8 sulfated) were >95% pure as evaluated by analytical reverse phase HPLC. The pH of the DPC micelle and water solutions were adjusted in between 4.5 and 5.8 by addition of 0.1 N NaOH and 0.1 N HCl; measurements were performed using an Orion model 601 pH meter fitted with a combination electrode for 5 mm NMR tubes (Ingold Electrodes, Wilmington, MA). Standard aqueous buffers were used for electrode calibration at pH 4 and 7.

Circular Dichroism and Fluorescence Studies. CD studies were performed on a Jasco J-710 spectropolarimeter at 25 °C. The sample concentrations of **1** and CCK-8(s) were 49 and 47 μM, respectively, in DPC solution (10 mM DPC in 50 mM phosphate buffer), which was freshly prepared immediately prior to acquisition of the spectra. Ten scans were averaged from 190 to 250 nm at a rate of 100 nm/min and the spectra were smooth. A 1.0 mm path length cell was used and the intensities are expressed as molar ellipticity $[\theta]$ (deg cm^2 dmol^{-1}). The CD instrument was calibrated using D-10 camphorsulphonic acid. After dissolving weighed amounts of dry powder in solution, the concentrations of the peptides in the samples were calculated by measuring the UV absorbance at 280 and using the molar extinction coefficients and the Beer−Lambert law equation.

Fluorescence emission spectra were recorded on a Photon Technology International spectrofluorimeter (Monmouth Junction, NJ). The concentrations of NATA, **1**, and CCK-8(s) were 49, 49, and 47 μM, respectively, in DPC solutions (10 mM DPC in 50 mM phosphate buffer) at pH 5.0. Because **1** is not soluble in aqueous solution, only the spectra in the presence of DPC micelles were collected for this peptide. These concentrations were calculated based on UV absorbance. Three scans of the emission spectra were recorded and averaged between 300 and 400 nm at 1 nm increments using a 1 mm quartz cell with a scan speed of 100 nm/min at room temperature. In these experiments, emission spectra were acquired with the excitation wavelength fixed at 280 nm with excitation and emission slit width set to 1 nm.

NMR Studies. NMR experiments were performed on a Bruker 600 MHz spectrometer in the City of Hope NMR facility with a 5 mm triple resonance *xyz*-gradient probe with the air temperature regulated at 35 °C. Solutions for NMR analysis of **1** and CCK-8(s) were made at approximately 2 mM peptide concentration in 750 μL of 90% H_2O/10% D_2O in with 100 mM DPC and 50 mM phosphate buffer present at pH 5.0. Chemical shift assignments for **1** and CCK-8(s) in micelle solution were obtained by the standard method[35] using total correlation spectroscopy (TOCSY[36]), nuclear Overhauser effect spectroscopy (NOESY[37]), and rotating-frame Overhauser effect spectroscopy (ROESY[38]) pulse sequences. All chemical shifts were reference to external 2,2-dimethyl-2-silapentane-5-sulfonic acid in D_2O.

Phase-sensitive NOESY data were used for conformational analysis of **1** and CCK-8(s) in DPC micelle solutions, with the Bruker library "noesyfpgpphrswg" pulse program.[39–41] A total of 8K points were collected in t2 (45 transients per increment), a 100 or 200 ms mixing time was used, and 480 complex points acquired in t1 using States-TPPI.[42,43] A relaxation delay of 1.9 s was used between transients. The transmitter channel was used for excitation and observation of the 6000 Hz proton frequency range. Water suppression was obtained by a Watergate sequence using flip-back pulses with radiation damping suppression via gradients in t1.[39] Data was processed with zero filling to 8K points in F2, 2K points in F1, and Gaussian, sine bell square apodization functions in both F1 and F2.

Phase-sensitive TOCSY spectra were collected to aide in the assignment of **1** and CCK-8(s) chemical shifts with the Bruker library "dipsi2esgpph" pulse program.[44,45] This pulse sequence performs homonuclear Hartmann−Hahn transfer using a DIPSI-2 sequence for mixing. Water suppression is performed using excitation sculpting with gradients. A total of 8K points were collected in t2 (24 transients per increment), a 45 and 70 ms mixing time were used, and 480 points were collected in t1 using States-TPPI. Data was processed with zero filling to 8K points in F2, 2K points in F1, and Gaussian and sine bell square apodization functions in both F1 and F2.

NMR Structure Calculations. Structures for **1** and CCK-8(s) were determined using XPLOR software, Version 3.1.[46] For **1** and CCK-8(s), 100 and 200 ms NOESY experiments provided the 59 and 53 distance restraints, respectively, needed for XPLOR 3D structure calculations. Distance restraints were input as 1.8 to 6.0 Å distance ranges and standard pseudoatom corrections were used where appropriate.[47] NOEs between protons within the same residue were not used except in cases where backbone to side chain distance constraints could influence the side chain orientation (e.g., for the Trp residues). The constraint set for **1** contained 3 intraresidue, 37 (i, $i+1$), 15 (i, $i+2$), and 4 (i, $i+3$) NOEs between protons on various residues and one angle constraint. For CCK-8(s), the set of constraints contained six intraresidue, 32 (i, $i+1$), 11 (i, $i+2$), and 4 (i, $i+3$) NOEs between protons on various residues and two angle constraints derived from $^3J_{NH\text{-}C\alpha H}$ values measured from 1D data.

These constraints were used for the calculation of **1** and CCK-8(s) structures, satisfying the distance boundaries. For **1**, 85 embedded-distance-geometry structures were obtained using the XPLOR ab initio simulated annealing protocol from a template coordinate set with a force constant of 50 kcal on the NOE-derived distance restraints. The parameter file "parallhdg.pro" was employed in this procedure. A thousand steps of conjugate-gradient energy minimization were applied to every coordinate set prior to writing to an output file. Once structures were generated in this fashion, they were subjected to an additional 10 ps of slow-cooling simulated annealing with softened van der Waals repulsion with a protocol

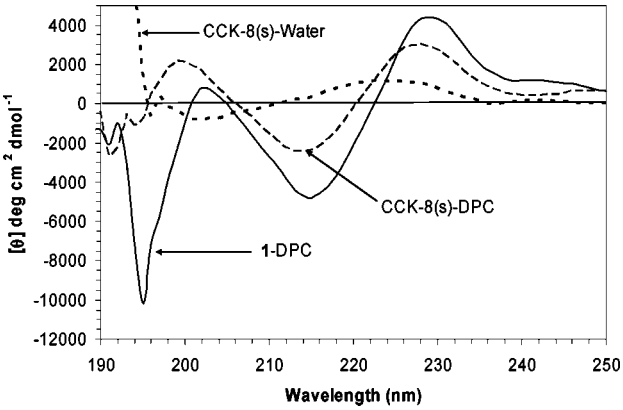

Figure 1. Plot of the CD molecular ellipticity from 190 to 260 nm of solutions 49 μM CCK-8(s) or **1** in water or in the presence of 10 mM DPC. All solutions were buffered with 50 mM sodium phosphate buffer at pH 5. The change in the pattern of the spectra indicates association of the peptide with the micelle with an alteration in the peptide conformation.

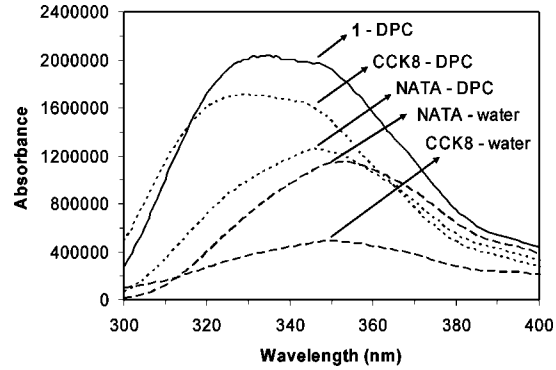

Figure 2. Plot of the fluorescence emission spectra from 300 to 400 nm after excitation at 280 nm of solutions of 49 μM CCK-8(s) or 47 μM NATA (*N*-acetyl tryptophan amide) in water alone and 49 μM CCK-8(s) or **1** or 47 μM NATA (*N*-acetyl tryptophan amide) in the presence of 10 mM DPC at pH 5 and 50 mM potassium phosphate buffer. The observed increase in CCK-8(s) and **1** fluorescence intensity in the presence of the lipid micelles is attributed to the insertion of the tryptophan indole rings into the hydrophobic lipid environs.

designed for NMR structure determination.[46,48] Out of the resulting 68 structures, 20 were chosen that had the lowest NOE restraint energies. Similarly for CCK-8(s), 199 embedded-distance-geometry structures were obtained using with the ab initio simulated annealing protocol for further slow-cooling simulated annealing refinement. Of the resulting 158 structures, 20 were chosen that had the lowest NOE restraint energies. X-PLOR generated structures were visualized with the program Insight (Version 2000, Accelrys, San Diego, CA). Root-mean-squared deviations (rmsds) were calculated with XPLOR for backbone (CO, CαH, NH atom positions only) or heavy (NH, CαH, CO, and side chain carbon, oxygen, and nitrogen) atom positions in a coordinate set versus the same atoms in the mean structure calculated from all coordinate sets. The use of distance constraints from 1.8 to 6 Å for the observed NOEs in the NMR data preferentially selects structures that comply with the longer distance constraints and de-emphasizes the importance of shorter i to $i + 1$ constraints. This method selects the folded conformations defined by the majority of the NOE derived distance constraints and puts less emphasis in the structure calculations on the larger NOE volumes observed in the spectra.

Results

CD Data. CD spectra from 190 to 250 nm are shown in Figure 1 for **1** or CCK-8(s) in DPC micelles at pH 5.0 (the pH where the NMR data was collected). The spectrum for CCK-8(s) in solution has one negative minima at 202 nm, a weak positive maximum at around 223 nm. These spectral features for CCK-8(s) in aqueous solution at pH 5.0 could describe a mixture of statistical-coil ([−]195−197 nm), β-turn (e.g., [+]190 and [−]213) conformers, and the contribution of the tryptophan indole ring orientation with respect to the peptide backbone ([+]230 nm).[49]

In the presence of DPC micelles, a conformational shift in CCK-8(s) occurs compared to the structure in aqueous solution (Figure 1). For CCK-8(s) in the presence of micelles, peaks at [−]190, [+]199, [−]214, and [+]228 nm are observed. The peak at 228 nanometers is characteristic of peptide tryptophan residues. Woody has observed that because of the low symmetry of the tryptophan side chain with respect to rotation about the χ2 bond (a dihedral formed by Cβ and Cγ carbons), the sign of the 230 nm band can change markedly with alterations in indole orientation.[50] Upon association with the DPC micelles, the CCK-8(s) indole moiety assumes an altered orientation with respect to the peptide backbone that causes a change in the wavelength and pattern of the peptides ellipticity. The peaks at [−]190, [+]199, and [−]214 are consistent with a turn structure with elements of statistical coil in the presence of micelles. Not observed are bands that would indicate the presence of residues in a purely helical ([+]195, [−]208, and [−]222 nm) or beta-sheet ([+]195 and [−]215 to 217 nm) conformation although these features can be obscured by the presence of the tryptophan ellipticity.[51,52]

For **1**, spectra were only obtainable in the presence of DPC micelles due to the limited solubility of this compound in water alone (Figure 1). The spectrum shares similarities to CCK-8(s) spectra in the presence of DPC micelles with peaks at [−]195, [+]202, [−]215, and [+]230 nm. However the intensity of these peaks is different for the two compounds; for example, the absolute difference of the [−]190 to [+]199 or [−]214 to [+]228 intensities in CCK-8(s) are 4890 or 5470 deg·cm^2·dmol^{-1}, while for **1**, the difference of [−]195 to [+]202 or [−]215 to [+]230 intensities are 11564 or 9180 deg·cm^2·dmol^{-1}. Thus, although the pattern of ellipticity is similar for the two peptides in the presence of DPC micelles, the altered peak intensities indicates some differences in the lipid associated structures.

Fluorescence Data. We compared the fluorescence of CCK-8(s) in solution or CCK-8(s) or **1** in the presence of DPC micelles, with NATA (*N*-acetyl tryptophan amide) to examine the effects of the different solution conditions on the environment of the tryptophan residues in CCK-8(s) or **1** relative to a mimic of an isolated tryptophan residue. The fluorescence emission spectra were recorded between 300 and 400 nm at an excitation wavelength of 280 nm. The spectra were collected on samples with 49 μM peptide or 47 μM NATA concentrations in water or in solution with 10 mM DPC micelles present at pH 5 and 50 mM in phosphate buffer. In Figure 2, CCK-8(s) or NATA in water have emission maximum of 349 and 354 nm, respectively. Because **1** has low solubility in water alone, no fluorescence spectra were collected for this sample. The intensity of the fluorescence of the tryptophan in CCK-8(s) in water alone is 3-fold less than that of NATA, indicating that folded conformers of CCK-8(s) in solution decrease the quantum yield of CCK W5 fluorescence compared to NATA.

In the presence of DPC micelles, the emission maxima for **1**, CCK-8(s), or NATA were blue-shifted to 335, 330, and 346 nm, respectively. In addition, a 350% increase in CCK-8(s) fluorescence was observed in the presence of micelles compared to CCK-8(s) in water alone. The intensity of the CCK-8(s)

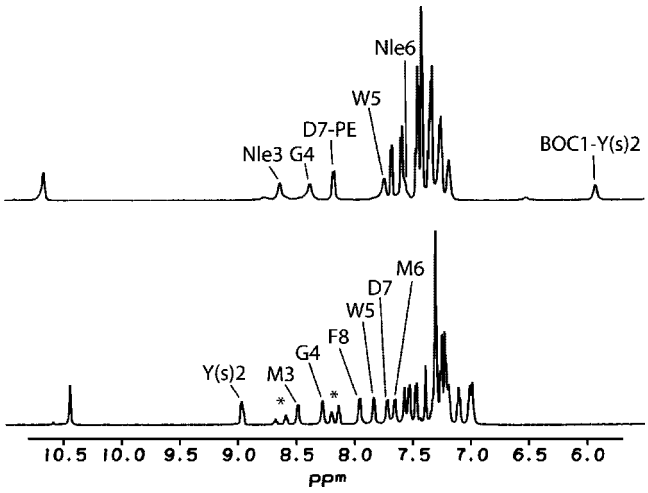

Figure 3. Portion of the 500 MHz 1D ^{1}H NMR spectrum from 5.5 to 11 ppm for 2 mM **1** (top) and CCK-8(s) (bottom) in the presence of 100 mM DPC micelles at 35 °C pH 5 and 50 mM in phosphate buffer. Peptide amide proton signals are labeled with their assignments. The asterisks denote signals from the presence of a pyridine impurity that was present in the DPC used in the CCK-8(s) sample.

emission maximum in the presence of DPC micelles is 20% greater than the **1** value. The intensity of the NATA fluorescence in the presence of DPC micelles also increased about 9% compared to its value in water alone, which may suggest some small association of NATA with the DPC micelles. These data are consistent with association of both peptides with DPC micelles with insertion of the W5 residues into a more hydrophobic environment.

NMR Data. A comparison of the 1D ^{1}H NMR spectra of **1** and CCK-8(s) is shown in Figure 3 in the presence of DPC micelles 50 mM phosphate buffer (pH 5) and 35 °C. At lower temperatures (25 and 15 °C), a second set of signals in slow exchange was observed for residues BOC-Y(s)2, Nle3, D7-PE, and the W5 indole NH, which decreased with increasing temperature and were mostly gone at 35 °C (data not shown). Therefore, structure data were collected at 35 °C for both peptides. Of note, comparison of the location of the amide proton signals of similar residues of CCK-8(s) and **1** shows that M3/Nle3 and G4 amide protons have similar chemical shift values, suggesting similar environments for these residues.

Essentially complete chemical shift assignments were obtained for **1** in the presence of DPC micelles (Figure 4a,b, Table 2). Complete chemical shift assignments for CCK-8(s) in water alone were available from previous studies.[53,54] In this work, the assignments of CCK-8(s) were determined in the presence of DPC micelles (Figure 4c,d, Table 2).

The chemical shifts of **1** or CCK-8(s) CαH protons in the presence of DPC micelles minus the statistical-coil solution-state chemical shifts of Wishart are plotted in parts a and b of Figure 5, respectively.[55,56] The statistical-coil chemical shifts of Wishart et al. were determined with short peptides (i.e., GGXAGG or GGXPGG, where X is one of the 20 AAs). Therefore comparison of these standard peptide CαH proton chemical shift values with CαH proton chemical shifts in CCK-8(s) or any other short peptide is informative in terms of comparison with statistical-coil structure. Of note, the Wishart et al. data set does not include nonstandard amino acids. Thus the presence of the sulfated tyrosine, Nle, BOC group, or phenylethylester is not controlled for in this comparison. With these caveats in mind, where the two peptides have similar residues (Nle3/M3-G4/G4), they have nearly identical NH and CαH proton chemical shifts except for a 0.22 ppm difference for the Nle3 and M3 CαH protons, which could be attributed to nonstandard AAs being present. Significant differences from statistical-coil values ($> \pm 0.1$ ppm) are observed for the CαH protons of residues M3, W5, M6, D7, and F8 for CCK8(s) and for BOC-Y(s)2 $C_\alpha H$ in **1**. For **1**, the unusual solution state chemical shift value for the Y(s)2 amide proton (5.78 ppm) is attributed to the proximity of BOC group (designated as residue BOC1) and the presence of DPC micelles.

For CCK-8(s), a comparison of the backbone $C_\alpha H$ and amide proton chemical shift values in water alone[53] and in the presence of DPC micelles reveals the effect of partitioning of the peptide onto the DPC micelle surface on the environment of these protons (Figure 5c). For CCK-8(s), significant changes in chemical shift values are observed for residues Y(s)2 through D7 with the largest differences in the amide proton values of M3 and M6 (+0.69 and −0.72 ppm, respectively, using $\delta_{DPC} - \delta_{H2O}$). Other notable changes in chemical shift values upon micelle association are the side chain protons of M3 β (+0.33 ppm) and γ (+0.45/+0.34 ppm), W5 β (+0.23/+0.38 ppm), W5 indole amide (+0.36 ppm), and M6 γ (−0.32/-0.33 ppm) and methyl (+0.30 ppm) protons.

1. For **1**, sequential $NH_{(i)}$ to $NH_{(i+1)}$ NOEs were observed in the 100 and 200 ms NOESY spectra between residues on Y(s)2, Nle3, G4, W5, Nle6, and D7 (Figures 5 and 6). Sequential $C\alpha H_{(i)}$ to $NH_{(i+1)}$ NOEs (which alternate between medium and strong intensities) were observed for Y(s)2, Nle3, G4, W5, Nle6, and D7. There were $d_{\alpha N}$ (i, $i + 2$) NOEs observed between Y(s)2 to G4 and Nle3 to W5, $d_{\beta N}$ (i, $i + 1$) Y(s)2 to Nle3, Nle3 to G4, W5 to Nle6, and Nle6 to D7, and $d_{\beta N}$ (i, $i + 2$) Y(s)2 to G4 and Nle3 to W5. Most of the observed strong, medium, and weak intensity NOEs were from (i, $i + 1$) with few (i, $i + 2$) or (i, $i + 3$) and no long-range NOEs were seen. These NOE data for **1** suggest some structure around residues 2−5 but the lack of longer range connectivities excludes extended secondary structure patterns (e.g., helices or β-sheets). Backbone scalar coupling constants were also measured from 1D NMR data. $^3J_{NH\text{-}C\alpha H}$ scalar coupling constant for **1** was in the range of 6.0−8.0 Hz, except Nle3, which has a value of 3.1 Hz.

CCK-8(s). Similar to **1**, 2D NOESY data on CCK-8(s) shows sequential $NH_{(i)}$ to $NH_{(i+1)}$ NOEs in the 100 and 200 ms spectra between residues Y(s)2, Nle3, G4, W5, Nle6, D7, and F8 (Figures 5 and 6). Furthermore, sequential $C_\alpha H_{(i)}$ to $NH_{(i+1)}$ NOEs (strong intensity) were observed for D1, Y(s)2, Nle3, G4, W5, Nle6, D7, and F8. Other NOEs were observed between $d_{\alpha N}$ (i, $i + 2$) Y(s)2 to G4, M3 to W5, and G4 to M6, $d_{\beta N}$ (i, $i + 1$) D1 to Y(s)2, Y(s)2 to M3, M3 to G4, W5 to M6, M6 to D7 and D7 to F8, $d_{\beta N}$ (i, $i + 2$) D1 to M3, and $d_{\beta N}$ (i, $i + 3$) Y(s)2 to W5, G4 to D7, and d_{NN} (i, $i + 2$) W5 to D7. In addition, the scalar coupling constant $^3J_{NH\text{-}C\alpha H}$ for CCK-8(s) were observed via 1D data in the range of 5.0−7.0 Hz with Y(s)2, M3, and M6 having values between 5 and 6 Hz. In comparison with the **1** data, there are several additional i, $i + 3$ NOE connectivities (residue 2−5 and residue 5−8) in the CCK-8(s) data that indicate differences in their micelle-associated structures. However, there are also several similar NOEs (e.g., $d_{\alpha N}$ (i, $i + 2$) Y(s)2 to G4, M3 to W5) that suggest these peptides may share similar backbone conformations in their N-termini.

Tertiary Structure Determination. 1. X-PLOR structure calculations were performed based on the NOEs derived from 100 and 200 ms NOESY spectra acquired on an aqueous solution of 2.0 mM **1** in 90% H_2O/10% D_2O (100 mM DPC in 50 mM phosphate buffer in pH 5.0). The NOEs were classified into medium (1.8−5.0 Å) and weak (1.8−6.0 Å) based on the

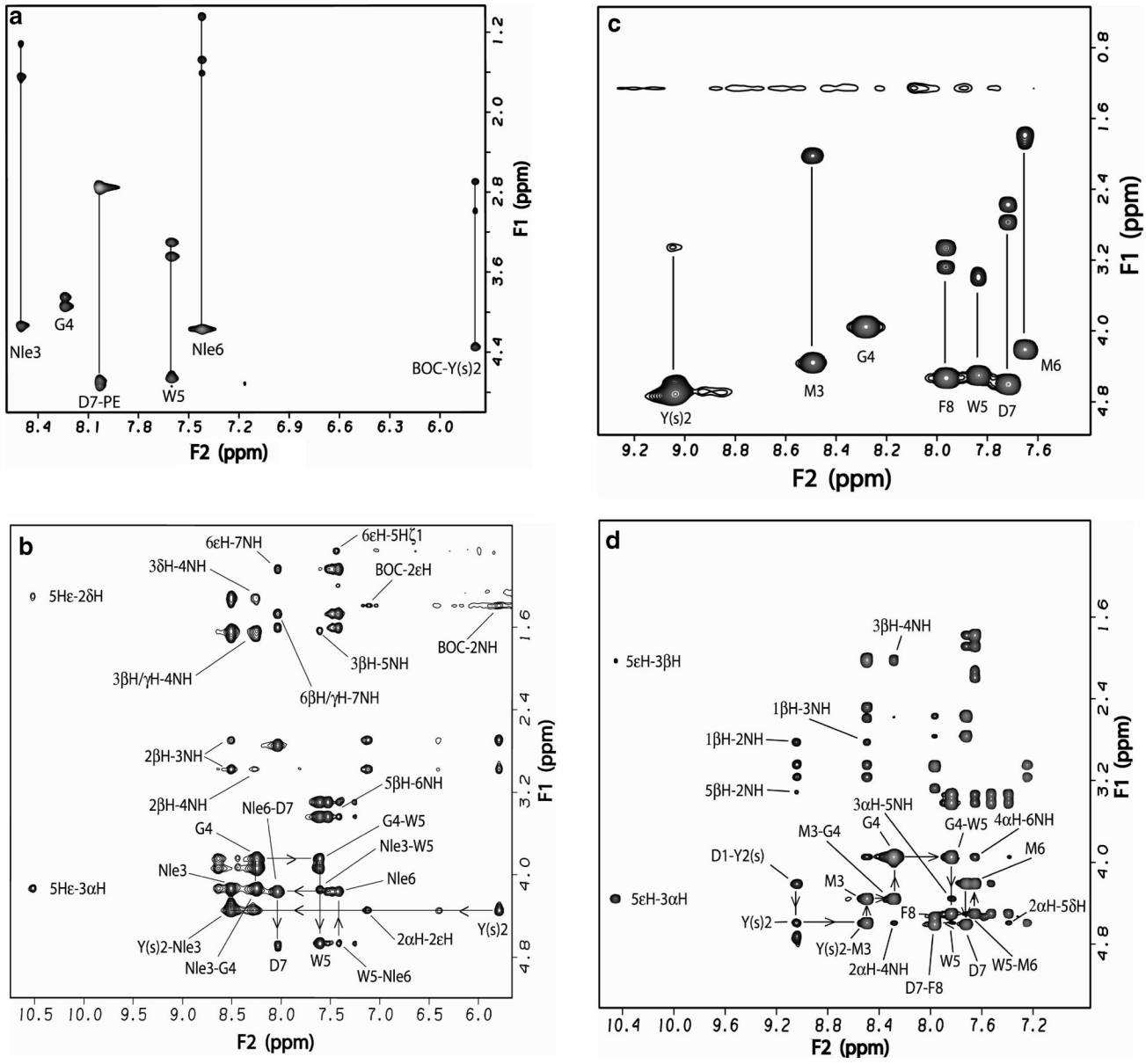

Figure 4. Homonuclear 600 MHz 2D ^{1}H NMR spectra acquired on a solution of 2 mM **1** or CCK-8(s), respectively, at pH 5.0 with 100 mM DPC and 35 °C in 90% H_2O/10% D_2O. (a,c) NH proton to CαH, CβH, CγH, and CδH proton correlation region of a 50 ms 2D TOCSY spectrum. (b,d) NH proton to CαH proton correlation region of a 200 ms 2D NOESY spectrum. Selected cross peaks are labeled and backbone CαH to NH connectivity denoted with lines and arrows.

intensity of the contour diagram. There were 59 NOEs derived distance constraints and one angle constraint that were used as an input file for the X-PLOR program to generated 85 initial structures by a simulated annealing protocol and further refined by molecular dynamics and energy minimization (see Materials and Methods).

Superpositions of the backbone atoms (NH, CαH, CO) of 20 or 10 coordinate sets were made from structures that had the lowest NOE restraint energies from a set of 68 structures that had no NOE violations greater than 0.3 Å. Figure 7 shows the backbone and heavy atom (NH, CαH, CO, and side chain carbon, oxygen, and nitrogen) RMSDs per residue for the overlay of 20 (backbone) or 10 (heavy atom) structures, respectively. The error bars denote the range of deviations from the mean structure for each residue of the 20 or 10 structure ensembles. Residues Y(s)2 and Nle3 are the most well defined, while Nle6 and D7-PE are the least precisely defined residue for both side chain and backbone atoms.

The calculated RMSDs for the 20 lowest energy structures were 0.55 ± 0.18 Å for the backbone atoms and 1.72 ± 0.34 Å for the heavy atom of residues 1−7 in **1**. For the 10 structure superposition, the rmsd for backbone and heavy atom RMSDs were 0.42 ± 0.11 and 1.45 ± 0.17 Å (Figure 8, red structures). Table 3 depicts the mean φ and ψ angles with standard deviations for the 20 lowest energy structures. The dihedral angles of Nle3 and G4 adopt type I β-turn (−60°, −30°, −90°, 0°), and the remaining amino acids are found in the extended conformation region of the Ramachandran plot.

CCK-8(s). X-PLOR structure calculations was performed based on the NOEs, which were derived for 100 and 200 ms NOESY spectra acquired on an aqueous solution of 2.0 mM CCK-8s in DPC micelle (100 mM DPC in 50 mM phosphate buffer in pH 5.0) at 35 °C. There were 53 NOE derived distance constraints and three angle constraint (Y(s)2, M3, and M6) used to generate 158 initial structures by a simulated annealing

Table 2. Chemical Shift Assignments of 2 mM **1** (top section) or CCK-8s (bottom section) in the Presence of 100 mM DPC, 50 mM pH 5 Phosphate Buffer at 35 °C

1	NH	$C_\alpha H$	$C_\beta H$	$C_\gamma H$	$C_\delta H$	others
BOC1						1.40
Y(s)2	5.78	4.35	2.98/2.69			7.18/7.11
Nle3	8.50	4.14	1.66	1.60	1.27	0.86
G4	8.24	3.93/3.85				
W5	7.61	4.66	3.45/3.33			2H = 7.25/4H = 7.53 5H = 7.04/6H = 7.10 7H = 7.44, NεH = 10.5
Nle6	7.43	4.17	1.57	1.44	1.20/1.16	1.00/0.82
D7-PE	8.04	4.68	2.74			PE = $CH_2-CH_2-C_6H_5$, na-na-2,6H = 7.24, 3,5H = 7.30, 4H = 7.26

CCK8(s)	NH	$C_\alpha H$	$C_\beta H$	$C_\gamma H$	$C_\delta H$	others
D1	NA	4.18	2.81/2.60			
Y(s)2	9.07	4.60	3.18/3.06			7.29, 7.19
M3	8.52	4.36	2.00	2.55/2.44		1.94
G4	8.31	3.96				
W5	7.87	4.51	3.43/3.35			2H = 7.42/4H = 7.55 5H = 7.04/6H = 7.14 7H = 7.50, NH = 10.48
M6	7.68	4.22	1.84	2.16/2.08		1.74
D7	7.75	4.62	2.77/2.58			
F8	7.99	4.54	3.29/3.07			7.34, 7.24, 7.22 $CONH_2$ = 7.60, 7.03

protocol and further refined by molecular dynamics and energy minimization (see Materials and Methods).

An overlay was produced of the 20 or 10 structures that had the lowest NOE restraint energies from a set of 158 structures that had no NOE violations greater than 0.3 Å after the last refinement step. Figure 7 shows the backbone and heavy atom RMSDs per residue for the overlay of 20 (backbone) or 10 (heavy atom) structures, respectively. The position backbone atoms are best defined at residues Y(s)2 and M3 and less precisely at the C-terminus. The side chain atoms of residue W5 is best defined, while Y(s)2, M6, and F8 side chains are the least precisely defined.

For the 20 structure superposition of CCK-8(s) coordinate sets, the calculated RMSDs are 0.75 ± 0.20 Å for the backbone atoms and 1.82 ± 0.34 Å for the heavy atom of residues 1−7. For 10 coordinate sets, the rmsd for backbone and heavy atom superposition are 0.64 ± 0.05 and 1.38 ± 0.17 Å. The mean dihedral angles of 20 structures show that Y(s)2 and M3 adopt helix-like φ, ψ angles (3_{10} helix, −60, −30, or classical helix −57, −47 degree consecutive residue $\varphi-\psi$ angles) (Table 3). However, frame shifting by one residue gives a type 1 β-turn (−60, −30, −90, 0) for residues M3 and G4. In addition, for CCK-8(s), there is a distorted helical-like sequence around M6 with residues W5 and D7 $\varphi-\psi$ angles falling outside of the classical geometry (Table 3). The dihedral angles of residues 3 and 4 of **1** and CCK-8(s) describe a type I β-turn for these residues in both peptides.

PROCHECK-NMR and AQUA are programs developed to examine the quality of structure calculated by NMR data.[57] The values of completeness and allowed $\varphi-\psi$ angle space inherent in PROCHECK-NMR are based on comparison with values derived from distance constraint sets and structures of peptides 17 amino acids or longer. After the structure calculations were completed we applied these programs to the analysis of the NOE derived distance restraints and the structure of CCK-8(s). A similar analysis for **1** is not possible due to the presence of the nonstandard amino acids in this peptide. For the 53 constraints used for CCK-8(s), 51 were found to be nonredundant by the AQUA criteria.

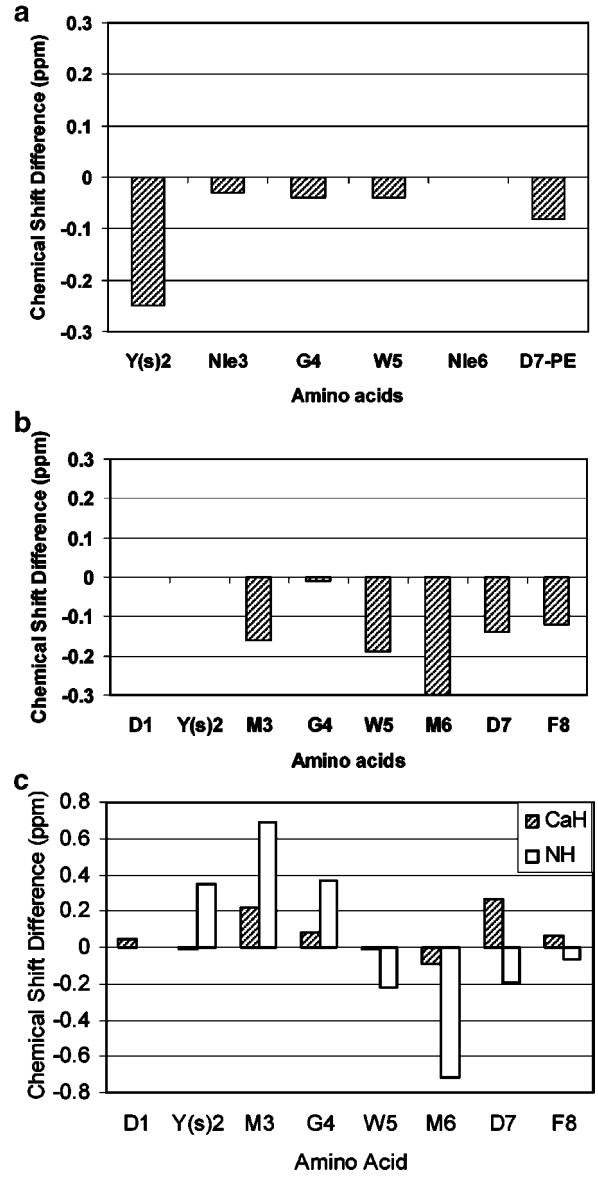

Figure 5. Chemical shift differences in the presence of DPC micelles. (a) A plot of the CαH chemical shift differences of **1** protons in the presence of DPC micelles versus the statistical-coil chemical shifts of Wishart et al.[77] (b) Plot of the CαH chemical shift differences of CCK-8(s) protons in the presence of DPC micelles versus the statistical-coil chemical shifts of Wishart et al.[77] (c) Plot of the chemical shift differences of the identical NH and CαH protons from CCK-8(s) in the presence of DPC micelles minus the chemical shifts of CCK-8(s) in aqueous solution.[53] Shift differences greater than ±0.1 ppm indicate a significant change in the chemical environment of the proton when going from aqueous to lipid milieus.

The PROCHECK analysis shows that the number of restraints per residue is sufficient to define the 3D structure of the peptide with good precision and accuracy. Clore et al. determined that the precision and accuracy of ensemble structures improves significantly as the number of interproton distance restraints is increased to an average of 15 per residue and improves incrementally less as more restraints are added above 15 per residue.[58] Residues M3, G4, M6, and D7 have 15 restraints-per-residue, while the greatest number was found for W5 with 30. These data also suggest that the structure is stable in the micelle environment because, generally, for NMR data, the greater the number of NOEs observed per residue the more restricted the range of motion for these residues in the peptide.

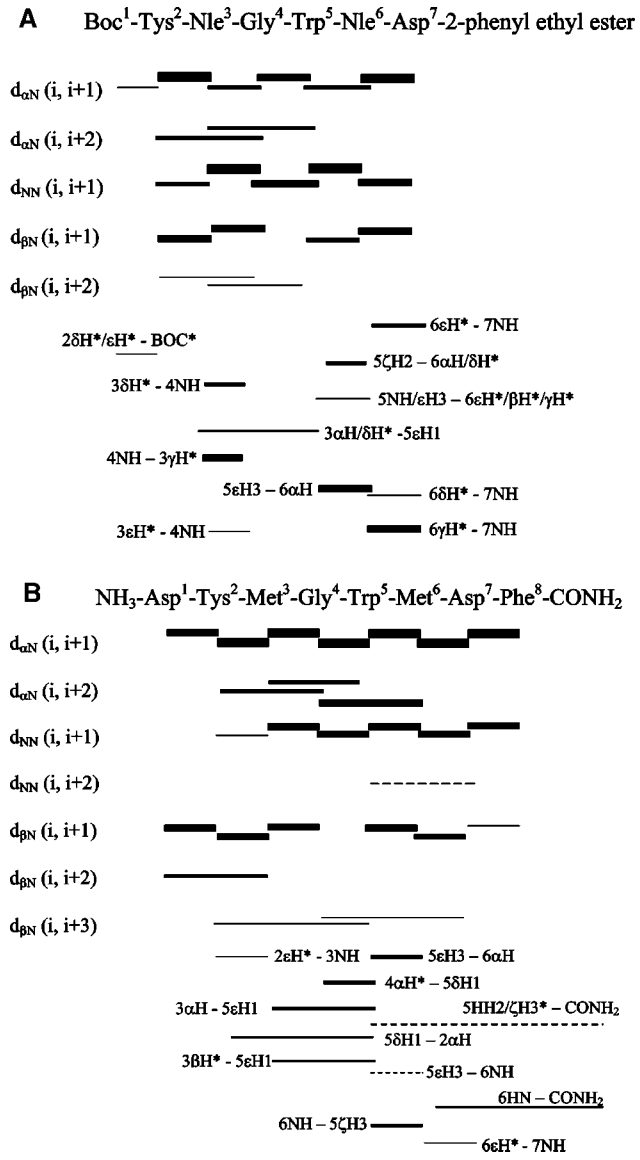

Figure 6. Selected NOE data used in the calculation of the tertiary structure of (A) **1** and (B) CCK-8(s). The intensity of the bar classifies the NOE as a strong, medium, or weak constraint. Selected NOE connectivity data is illustrated. The asterisk denotes that a pseudoatom correction was used for the connectivity shown.

The AQUA completeness score for CCK-8(s) is 19.8%, with residues M3−F8 having the best scores (completeness 20−35%). For the N-terminal portion of the peptide, residues D1 and Y(s)2 had completeness scores of 10−15%. The Ramachandran analysis of the 20 lowest NOE restraint energy structures (160 residues total) shows 29% of the $\varphi-\psi$ angles in the most favored region, 57% in additionally allowed region, and another 13% for the generously allowed region of the plot.

For comparison, 3D structure studies of similarly sized peptides reveals that the number of restraints we report here is very similar to literature values (e.g., refs 19, 59, 60). For example, an 11 amino acid peptide called SPA had a completeness score of 13%, with the best defined portion having 20−25% values and 65 nonredundant distance constraints.[19] For this study, the presence of the long-range NOE cross-peaks is unequivocal and our calculated structure represents a conformation that satisfies the complete sets of distance restraints without violation of a single distance bounds by the XPLOR criteria for both peptides.

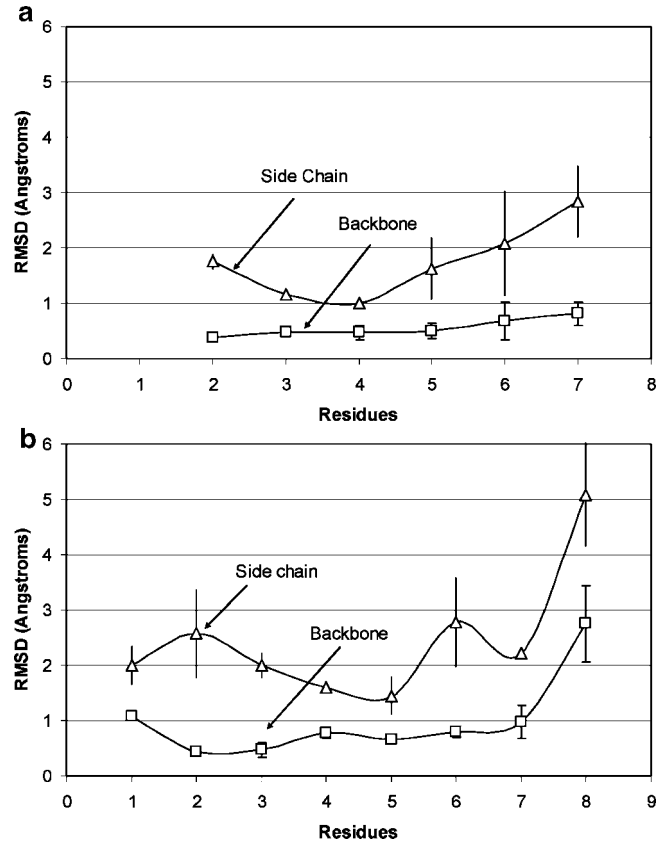

Figure 7. Plots of the rmsd per residue for the backbone (empty squares) and heavy atom (empty triangles) superposition of (A) **1** or (B) CCK-8(s) of the 20 backbone or 10 heavy atom X-PLOR-calculated structures. The error bars denote the range of deviations from the mean structure for each residue of the 20 or 10 structure ensembles.

Discussion

The structures of CCK-8(s) and its analogue **1** associated with DPC micelles determined by NMR methods share a common element from residue Y(s)2 to W5, but diverge in residues M6, D7, and F8. These structures may reflect the conformation of the peptides as they interact with the cell membrane before they encounter the CCK_1 receptor. The C-terminal CCK-4 (WMDF-amide) sequence is the minimum sequence required to function as cholecystokinin.[1] CCK_1 receptor specificity is enabled by N-terminal extension to sulfated CCK-7.

For a DPC micelle-associated structure to provide de novo information of a CCK_1 receptor bound conformation, the 3D structural elements should be mimicked in the lipid environment. Intuitively one would not expect the structure of the receptor-bound ligand and a lipid-associated ligand to mimic each other conformationally because of the many differences in the properties of receptor amino acids and lipid headgroups. However, we show here that both CCK-8(s) and **1** share a common structural element with Miller's CCK_1 receptor-bound model of CCK-8(s). We suggest that this result and those observed with the PACAP receptor support the hypothesis that at least some part of the ligand−receptor interaction for these peptides is mediated via a lipid-membrane-bound pathway for the ligand.

The similarities and differences in tertiary structures of **1** and CCK-8(s) are attributed to their primary sequence similarities and differences. For **1**, the presence of the BOC and phenyl-

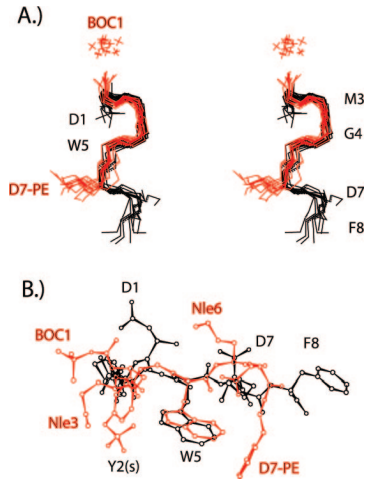

Figure 8. Stereo view of (A) the superposition of 10 coordinate sets of the backbone atoms of residues 1−7 of **1** (red) or CCK-8(s) (black). For **1**, the rmsd for backbone and heavy atom superposition are 0.42 ± 0.11 and 1.45 ± 0.17 Å, respectively. The figure shows the superposition of the backbone atoms of residues 2−5 of **1** (red) onto residues 2−5 of CCK-8(s) (black) for each similarly numbered pair of coordinate sets. For CCK-8(s), the rmsd for backbone and heavy atom superposition are 0.64 ± 0.05 and 1.38 ± 0.17 Å, respectively. The rmsd for the superposition of the backbone atoms of the **1** mean structure onto the CCK-8(s) mean structure (mean of 10 coordinate sets each) is 0.91 Å. (B) The superposition of the backbone atoms of residues 2−5 of **1** (red) on to the same atoms of CCK-8(s) (black) for one coordinate set with the heavy atoms shown (rmsd 0.98 Å). These overlays show that **1** and CCK-8(s) in the presence of DPC micelles share similar backbone structures from residue Y(s)2 to W5 and diverge from each other at D1/BOC, M6/Nle6, D7/D7, and F8/-PE.

Table 3. Mean φ and ψ Angle for the 20 Lowest Energy Structure of **1** and CCK-8(s) Derived from XPLOR Program Structures

	1		CCK-8(s)	
dihedral angle	φ (deg)	ψ (deg)	φ (deg)	ψ (deg)
Y(s)2	−125 (±29)	21 (±13)	−47 (±15)	−32 (±24)
Nle3 (or) M3	−40 (±10)	−30 (±20)	−85 (±6)	−37 (±34)
G4	−98 (±10)	9 (±14)	−124 (±26)	0 (±22)
W5	−25 (±14)	137 (±28)	−6 (±35)	−133 (±38)
Nle6 (or) M6	−121 (±17)	−4 (±11)	−66 (±13)	−67 (±17)
D7			−74 (±28)	19 (±30)

ethylester groups makes the N-and C-termini more hydrophobic than the corresponding amino and amide groups of CCK-8(s), and upon association with a lipid surface, these residues adopt alternate conformations. By contrast, the similarity of the Y2(s), M3/Nle3, G4, and W5 residues enables similar turn structures to form in the presence of the micelles. The environment of the CCK_1 receptor in the Miller model induces an identical type I turn in CCK-8(s). An important caveat to this observation is that our structures do not conform to those observed by Fourmy's group based primarily on site-directed mutagenesis studies or those of Meirke's that are based on NMR studies using micelles with receptor fragments present. As more evidence is gathered and these models converge on the true receptor-bound ligand conformation, these comparisons should be re-evaluated.

Importantly, the DPC micelle-associated structures derived here may be of use for structure-based drug design not only because they may directly mimic receptor-bound conformations but they may also act indirectly to alter membrane properties that modulate receptor function. The lipid membrane is a 2D solvent in which the GPCRs exist and interact with both extracellular and intracellular ligands. Therefore, changes in the properties of the membrane (e.g., viscosity, solvation, and charge state) caused by ligand association could have a strong effect on the dynamic equilibrium of a GPCR between active and inactive states[61] as well as G-protein coupled states.[62] In this manner, a cell can respond to external stimuli by triggering signal transduction cascades elicited by ligands interacting directly with their receptors but also by indirect modulation of receptor function via ligands associating with the membrane surface away from the receptor site.

The lipid microenviroment has been shown to be important for the function of several receptors. In the case of the CCK_1 receptor, Harikumar et al. has shown that ligand binding, signaling, internalization, and receptor trafficking activity are sensitive to the membrane lipid composition and likely to the lipid microenvironment of the receptor (e.g., the presence of varying amounts of cholesterol or sphingolipids).[63] Similarly, cholesterol depletion alters membrane characteristics and changes $serotonin_{1A}$ receptor function.[64] Furthermore, the bradykinin-2 receptor has been shown to change conformation when stimulated by factors that alter the membrane fluidity (e.g., sheer stress, hypotonic shock, benzyl alcohol, or the presence of bradykinin).[65] In addition, peptides such as melittin are known to potently change membrane properties at low peptide concentrations (e.g., ref 66). Finally, we note that this membrane mediated GPCR modulator mechanism could enable one peptide to act as an antagonist at multiple peptide hormone receptors by altering membrane properties that influence the function of multiple receptor types. This type of multireceptor antagonist activity is observed for the broad-spectrum-neuropeptide-antagonist family of peptides, which are a class of tryptophan-rich therapeutic compounds with anticancer properties (e.g., ref 19 and references therein).

In this work, we examine the DPC micelle associated structures of **1** and CCK-8(s) because some have theorized that cell membranes mediate the transport of peptide ligands toward their receptors and the 3D conformation of the ligand that binds and activates the receptor.[21–23] There is specific evidence that gastrin[67–70] and CCK[15,16,71–75] molecular forms interact with the CCK_1 or CCK_2 receptor via such a lipid-associated mechanism. The common element from residue Y(s)2 to W5 in CCK-8(s) and **1** may be the element that interacts with the cell membrane and mediates the transport of these peptides toward their receptors.

To validate the use of DPC micelles as a proxy for receptor-bound conformations of peptide ligands requires an example where the receptor-bound conformation is known. Unfortunately, for almost all peptide ligand−GPCR complexes, the conformation of the ligand bound to the receptor is not known. However, in the case of cholecystokinin and **1**, there are several receptor-bound models carefully developed from mutagenesis, cross-linking, or NMR data that can be used for comparison with the structures determined in this work in the presence of DPC micelles. To develop a detailed and self-consistent comparison for these ligands, we probed the conformation of CCK-8(s) or **1** in the presence of DPC micelles by CD, fluorescence, and NMR methods.

Circular Dichroism. The CD data for **1** and CCK-8(s) collected in the presence of DPC micelles shows bands characteristic of turn structures ([−]214−215 nm) and the tryptophan indole ring orientation contribution ([+]228−230 nm) (Figure 1). In addition, the spectral features for CCK-8(s) in water alone are very different from those observed in the presence of DPC micelles, indicating a large change from the solution state population of folded conformers that have been

proposed for CCK-8 in water alone (Table 1). Thus these data suggest that CCK-8(s) and **1** partition into DPC micelles in a turn conformation with insertion of the W5 indole moiety.

Fluorescence Data. The fluorescence data obtained with excitation at 280 nm for **1**, CCK-8(s), or NATA are consistent with the CD data (Figure 2). CCK-8(s) fluorescence emission intensity is blue-shifted and increased compared to water alone in the presence of DPC micelles consistent with the insertion of the W5 indole moiety into a more hydrophobic environment. By contrast, a trytophan indole mimic, NATA, shows only a minor change in the presence of the micelles, indicating little partitioning of this compound into the lipid. Thus the partitioning of the peptides into the DPC micelles is a property of their sequence and not driven wholly by the known energetically favorable interaction of tyrptophan residues with the interfacial region of lipid bilayers.[76]

NMR. The NMR data obtained on **1** or CCK-8(s) (Tables 2 and 3 and Figures 4, 5, 6, and 7) yield detailed chemical shift and NOE information on individual protons. A plot of the CαH chemical shift differences of **1** protons in the presence of DPC micelles versus the statistical-coil chemical shifts of Wishart et al.[77] show a large change from statistical-coil conformation only at the BOC group adjacent Y(s)2 residue, while for CCK-8(s), there are differences at M3 and W5 to the C-terminus of the peptide (parts a and b of Figure 5, respectively). We interpret this as an extended chain-like conformation for the C-terminal residues of **1** while CCK-8(s) has additional nonstatistical-coil structure. However, comparison with statistical-coil chemical shifts may not be valid for **1** because of the presence of altered amino acids (e.g., BOC-Y, Nle, and D-PE) whose CαH chemical shifts have not been characterized in statistical-coil model peptides.

The NMR chemical shift data collected on CCK-8(s) in the presence of DPC micelles show a major shift in tertiary structure compared to water alone (Figure 5c). This comparison is between identical protons in the two environments and large changes ($\geq \pm 0.2$ ppm) are observed from Y(s)2 to D7 (Figure 5c). These data suggest that the partially folded structure in aqueous solution binds the DPC micelles with an insertion of W5 residues into the micelle with changes in environment centered on M3 or M6.

1. For **1** in the presence of DPC, micelles fold into a unique tertiary structure. This fold is stable enough for the observation of intermolecular NOEs and chemical shift perturbations. The long-range NOEs in Figure 6 and the other NOEs observed in 100 and 200 ms NOESY data were used to calculate the structure observed in Figure 8 (red structures). No helical-like $\varphi-\psi$ backbone geometry is observed (a classical helix would have consecutive $\varphi-\psi$ angle pairs of -57 and -47 degrees and a 3_{10} type helix would have $-60°$, $-30°$ consecutive $\varphi-\psi$ angles, Table 3). The structure can be described as a type I turn around residues Nle3 and G4 (Type I: residue 2 $-60°$, $-30°$, residue 3 $-90°$, $0°$ $\varphi-\psi$ pairs) with the C-terminal residues in an extended conformation.

The precision of the overlay indicates the tertiary structure of the backbone for residues Y(s)2 to D7-PE are well defined ($\leq$1 Å) with the orientation of the side chains established best for Y(s)2, G4, Nle3, and W5 ($\leq$2 Å) (Figure 7a). The position of the side chains of residues Nle6 and D7-PE are less well defined ($\geq$2 Å) by NOE distance constraints compared to neighboring residues.

CCK-8(s). The long-range NOEs in Figure 6 and the other NOEs observed in 100 and 200 ms NOESY data were used to calculate the structure observed in Figure 8 (black structures). The structure can be described has a type I turn around residues M3 and G4, with the C-terminal residues W5, M6, and D7 having a distorted helical geometry (Table 3). We call this a distorted helical geometry because while the backbone dihedral angles of M6 are helix-like, the preceding and following residues fall outside of the classical or 3_{10} helical angles. The precision of the superposition indicates the tertiary structure of the backbone for residues Y(s)2 to D7 are well defined ($\leq$1 Å) with the orientation of the side chains established best for D1, M3, G4, and W5 (Figure 7b). The position of the side chains of residues Y(s)2, M6, D7, and F8 are less well defined by NOE distance constraints compared to neighboring residues.

Summary of 1/DPC and CCK-8(s)/DPC Conformations. Figure 8 shows that **1** and CCK-8(s) in the presence of DPC micelles share similar backbone structures from residue Y(s)2 to W5 and diverge from each other at D1/BOC, M6/Nle6, D7/D7, and F8/-PE. The structural data presented in Figure 8 is consistent with the CD, NMR, and fluorescence data. Of note, the CD data is not consistent with the presence of a predominantly helical peptide. CCK-8(s) does appear to have a tendency to form a helix in DPC micelles, indicated by the observation of some helix like angles in the NMR derived structures. However, in our NOE data, the M3-G4 type I turn predominates, is well defined in both calculated structures and in the CD spectrum.

The W5 indole moiety in **1** and CCK-8(s) is found in a similar orientation relative to the peptide backbone atoms. Tryptophan residues are known to home to the water−lipid interfacial region of membranes.[76,78] The fluorescence data shows that NATA alone does not partition significantly into DPC micelles, thus the properties of the surrounding residues of each peptide (e.g., the type I turn formed around M3/Nle3 and G4) must also play a role in the peptide−micelle association.

Comparison to Literature CCK/DPC Structures. The type I β-turn containing residues Y(s)2, Nle3/M3, G4, and W5 of CCK-8(s) in the presence of DPC micelles differs from the helical type structures that have been presented in the literature (Table 1). Pellegrini and Mierke determined the structure of CCK-8(ns) in DPC micelles by combining 150 ms NOESY data at three different temperatures (298, 308, and 318 K) with a pH of 6.5 (Table 1). Our NOE data on CCK-8(s) was acquired at 100 and 200 ms mixing times in the presence of DPC micelles, 308 K, pH 5, and 50 mM phosphate buffer. Pellegrini and Mierke used 64 total NOEs in their DG-MD structure calculation consisting of 30 intraresidue, 19 $i, i+1$, 6 $i, i+2$, 6 $i, i+3$, and 3 $i, i+4$, while our XPLOR data set of 53 constraints contains 6 intraresidue, 32 $i, i+1$, 11 $i, i+2$, and 4, $i, i+3$, NOEs. Our computational approach focuses on the inter-residue NOEs and excludes most intraresidue NOEs because most proton to proton distances within an amino acid fall inside the range of distances allowed by our constraint set. In our calculations, intraproton distance restraints are only used for residues like tryptophan where backbone-to-side chain NOEs could provide information on the orientation of the side chain. For the $\geq i, i+2$ NOEs, our data set and Pellegrini and Mierke's data set contain crosspeaks between protons on D1 and M3, D1 to G4, Y2/Y2(s) and G4, Y2/Y2(s) and W5, G4 and M6, G4 and D7, and M6 and F8. We observe seven $i, i+2$ NOEs between protons on M3 and W5 or W5 and D7 not observed in Pellegrini and Mierke's data set. By contrast, Pellegrini and Mierke observed crosspeaks between M3 to M6, M3 to D7, and G4 to F8 protons that we do not observe. These comparisons suggest that the structural differences observed in the calculated structures results from differences in the NOE data acquired.

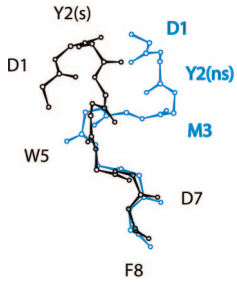

Figure 9. Comparison of the DPC micelle bound structures CCK-8(s) with the Mierke group model of receptor bound CCK-8(ns): Backbone atoms of CCK-8(ns) in the presence of DPC micelles with the N-terminal 1−47 residues of the CCK_1 receptor (blue structure, Mierke's laboratory PDB coordinate set 1D6G) are superposed on the same atoms in residues 5−8 of CCK-8(s) in DPC micelles (black structure). The rmsd for superposition of 1D6G onto CCK-8(s) residues 5−8 is 0.64 Å.

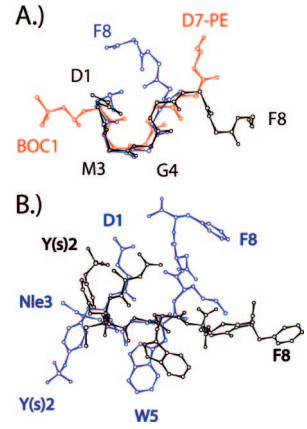

Figure 10. Comparison of the DPC micelle bound structures of **1** (red) or CCK-8(s) (black) with the Miller group model of receptor bound [$Nle^{3,6}$]CCK-8(s) (purple):[32] (A) The superposition of the backbone atoms of residues 2−5 of **1** or CCK-8(s) gives RMSDs of 1.01 or 0.86 Å, respectively. (B) A heavy chain representation of the Miller group [$Nle^{3,6}$]CCK-8(s) and CCK-8(s) in the presence of DPC structures superposed at backbone atoms for residues 2−5: The position of the side chain heavy atoms is also very similar for D1/D1, M3/Nle3, G4/G4, and W5/W5. The side chain position of Y(s)2 is very different as are the backbone and side chains from M6/Nle6 to the C-terminus.

These NOE differences could arise due to the higher pH used in Mierke's study, although both aspartate residues would be mostly titrated at pH 5 and above if the micelle associated pK_a's for these residues is around 4. In addition, the range of temperatures used could yield additional NOEs that we did not observe at one temperature. The other obvious difference is the presence of the sulfate group on the tyrosine in position 2. However Giragossian et al. report a similar structure to CCK-8(ns) for CCK-15(s) in the presence of DPC micelles at pH 5, which argues against the importance of the sulfate group, N-terminal extension, or pH in the 3D structure determined. We conclude that our NOE data and that of Pellegrini and Meirke may differ because of differences in experimental detail.

In this work, because the structure of CCK-8(s) and **1** may be sensitive to the solution conditions used, we compare data sets acquired on these two potent CCK_1 analogues under identical solution conditions. In addition, we collected CD data to corroborate the secondary structure elements present in these peptides under conditions similar to those used for the NMR analysis. Thus, we have self-consistent data on CCK-8(s) and **1**, which show a very similar type I β-turn and diverge from each other at the N- and C-termini. Importantly, the CD data for CCK-8(s) or **1** in the presence of DPC micelles does not show helical character but rather is consistent with the β-turn conformation that is observed in the structure calculated from our current NMR data.

Comparison of 1/DPC or CCK-8(s)/DPC Structures with Available CCK_1 Receptor Bound Models. Figures 9 and 10 illustrate the important comparisons of the DPC micelle bound structures of **1** and CCK-8(s) determined in this work with three available models of CCK_1 receptor bound **1**, CCK-8(s), or CCK-8(ns).[16,32,34] In Figure 9, backbone atoms of CCK-8(ns) in the presence of DPC micelles with the N-terminal 1−47 residues of the CCK_1 receptor present (blue structure, Mierke laboratory PDB coordinate set 1D6G[16]) are superposed on the same atoms in residues 5−8 of CCK-8(s) in DPC micelles (black structure). The RMSDs for superposition of 1D6G onto CCK-8(s)/DPC residues 1−8, 4−8, or 5−8 are 2.55, 1.24, or 0.64 Å, respectively. Thus there is a common C-terminal structural element in the Mierke group model and the structure of CCK-8(s)/DPC determined in this work. These structures show N-terminal divergence that may be caused by the presence of a portion of the CCK_1 receptor, the absence of the sulfate group, or the solutions conditions used to collect the data.

Visual comparison of residues 2−5 of the **1** model created by the Fourmy group (Figure 5a,b in ref 34) and the same atoms of **1** in the presence of DPC micelles show poor structural homology. Fourmy's group published a comparison of the structure of CCK-8(s) when bound to the CCK_1 receptor superposed onto the Mierke group DPC associated structure and reported a rmsd of 2.4 Å (Figure 7 in ref 33). If the Fourmy group or Meirke laboratory models are correct, these comparisons give a measure of how precisely the DPC micelle associated structure of these peptides matches that of a receptor bound form.

Figure 10 illustrates the comparison of CCK-8(s) or **1** determined in this work with [$Nle^{3,6}$]CCK-8(s) bound to the CCK_1 receptor developed in the Miller laboratory.[32] The Miller group model differs from that developed by Fourmy's group in that it contains a β-turn at Nle3-G4 which juxtaposes the N-terminal aspartate residue with the C-terminal phenylalanine residue. By contrast, in the Fourmy group model these residues are separated in an extended helical conformation. Remarkably, superposition of backbone atoms of residues 2−5 of the Miller group structure of [$Nle^{3,6}$]CCK-8(s) bound to CCK_1 with the same atoms in our **1** or CCK-8(s) (Figure 10a) structures give RMSDs of 1.01 or 0.86 Å, respectively. In addition, for CCK-8(s) the side chain moieties of D1, Nle3/M3, G4, and W5 are found in similar alignments in that model and in our current NMR data (Figure 10b).

Conclusions

The energetics of the association of peptide ligands with lipid membranes or a receptor in a cell surface are governed by multiple parameters, including: peptide secondary structure, peptide orientation, desolvation of both ligand and receptor residues with binding, and alteration of lipid or receptor characteristics upon ligand association. The complexity of this interaction makes distinguishing what parameters are most important for facile peptide−receptor interaction a difficult task. In this work, we have used a model lipid system in the absence of the receptor to compare two peptide ligands that act on the same receptor in both different and the same fashion. We find that the peptides have a region of overlapping structure and diverge in other areas that could theoretically explain their unique activities.

The DPC micelle-associated ligand model enables molecular level detailed structures to be obtained by NMR methods at a water-bilayer-like interface where determining structure in the presence of a cell surface receptor is very difficult with current technology. In the case of **1** and CCK-8(s), there are several carefully constructed models of interactions of these peptides with the CCK_1 receptor from the research groups of Fourmy, Miller, and Mierke that can be used to test the validity of the DPC model as a surrogate for receptor-bound structure. For CCK-8(s) and **1**, we conclude that DPC micelle associated structures do predict the conformations of important residues for CCK_1 receptor binding and activation. However, we note that the comparisons in this work are only as valid as the models of these analogues bound to the CCK_1 receptor. As new structural data, cross-linking, and mutagenesis results are incorporated, these models should ultimately converge on a structure or structure(s) that explain all the available experiment detail, the comparison with the DPC micelle associated structures should be revisited.

Acknowledgment. This work was supported in part by the CURE Digestive Diseases Research Center Grant (DK 41301), NIH grant DK33850 (J.R.R.), NIH Grant DK32878 (L.J.M.), and the Medical Research Service of the Veterans Health Service.

References

(1) Reeve, J., Jr.; Eysselein, V. E.; Ho, F. J.; Chew, P.; Vigna, S. R.; Liddle, R. A.; Evans, C. Natural and synthetic CCK-58. Novel reagents for studying cholecystokinin physiology. *Ann. N.Y. Acad. Sci.* **1994**, *713*, 11–21.

(2) Matozaki, T.; Martinez, J.; Williams, J. A. A new CCK analogue differentiates two functionally distinct CCK receptors in rat and mouse pancreatic acini. *Am. J. Physiol.* **1989**, *257* (4 Pt 1), 594–600.

(3) Sato, S.; Stark, H. A.; Martinez, J.; Beaven, M. A.; Jensen, R. T.; Gardner, J. D. Receptor occupation, calcium mobilization, and amylase release in pancreatic acini: effect of CCK-JMV-180. *Am. J. Physiol.* **1989**, *257* (2 Pt 1), G202–G209.

(4) Stark, H. A.; Sharp, C. M.; Sutliff, V. E.; Martinez, J.; Jensen, R. T.; Gardner, J. D. CCK-JMV-180: a peptide that distinguishes high-affinity cholecystokinin receptors from low-affinity cholecystokinin receptors. *Biochim. Biophys. Acta* **1989**, *1010* (2), 145–150.

(5) Asin, K. E.; Bednarz, L. Differential effects of CCK-JMV-180 on food intake in rats and mice. *Pharmacol. Biochem. Behav.* **1992**, *42* (2), 291–295.

(6) Williams, J. A.; Blevins, G. T., Jr. Cholecystokinin and regulation of pancreatic acinar cell function. *Physiol. Rev.* **1993**, *73* (4), 701–723.

(7) Saluja, A. K.; Lerch, M. M.; Phillips, P. A.; Dudeja, V. Why Does Pancreatic Overstimulation Cause Pancreatitis? *Annu. Rev. Physiol.* **2006**, *69*, 249–269.

(8) Dockray, G.; Dimaline, R.; Varro, A. Gastrin: old hormone, new functions. *Pflugers Arch.* **2005**, *449* (4), 344–355.

(9) Galas, M. C.; Lignon, M. F.; Rodriguez, M.; Mendre, C.; Fulcrand, P.; Laur, J.; Martinez, J. Structure−activity relationship studies on cholecystokinin: analogues with partial agonist activity. *Am. J. Physiol.* **1988**, *254* (2 Pt 1), G176–G182.

(10) Yule, D. I.; Tseng, M. J.; Williams, J. A.; Logdson, C. D. A cloned CCK-A receptor transduces multiple signals in response to full and partial agonists. *Am. J. Physiol.* **1993**, *265* (5 Pt 1), G999–G1004.

(11) Ji, B.; Kopin, A. S.; Logsdon, C. D. Species differences between rat and mouse CCKA receptors determine the divergent acinar cell response to the cholecystokinin analog JMV-180. *J. Biol. Chem.* **2000**, *275* (25), 19115–19120.

(12) Poosti, R.; di Malta, L.; Gagne, D.; Bernad, N.; Galleyrand, J. C.; Escrieut, C.; Silvente-Poirot, S.; Fourmy, D.; Martinez, J. The third intracellular loop of the rat and mouse cholecystokinin-A receptors is responsible for different patterns of gene activation. *Mol. Pharmacol.* **2000**, *58* (6), 1381–1388.

(13) Saluja, A. K.; Saluja, M.; Printz, H.; Zavertnik, A.; Sengupta, A.; Steer, M. L. Experimental pancreatitis is mediated by low-affinity cholecystokinin receptors that inhibit digestive enzyme secretion. *Proc. Natl. Acad. Sci. U.S.A.* **1989**, *86* (22), 8968–8971.

(14) Fournie-Zaluski, M. C.; Belleney, J.; Lux, B.; Durieux, C.; Gerard, D.; Gacel, G.; Maigert, B.; Roques, B. P. Conformational analysis of cholecystokinin CCK26-33 and related fragments by ^{1}H NMR spectroscopy, fluorescense-transfer measurements, and calculations. *Biochemistry* **1986**, *25*, 3778–3787.

(15) Giragossian, C.; Mierke, D. F. Intermolecular interactions between cholecystokinin-8 and the third extracellular loop of the cholecystokinin A receptor. *Biochemistry* **2001**, *40* (13), 3804–3809.

(16) Pellegrini, M.; Mierke, D. F. Molecular complex of cholecystokinin-8 and N-terminus of the cholecystokinin A receptor by NMR spectroscopy. *Biochemistry* **1999**, *38* (45), 14775–14783.

(17) McDonnell, P. A.; Opella, S. J. Effect of detergent concentration on multidimensional solution NMR spectra of membrane proteins in micelles. *J. Magn. Reson., Ser. B* **1993**, *102*, 120–125.

(18) Kallick, D. H.; Tessmer, M. R.; Watts, C. R.; Li, C. Y. The use of dodecylphosphocholine micelles in solution NMR. *J. Magn. Reson., Ser. B* **1995**, *109*, 60–65.

(19) Keire, D. A.; Kumar, M.; Hu, W.; Sinnett-Smith, J.; Rozengurt, E. The lipid-associated 3D structure of SPA, a broad-spectrum neuropeptide antagonist with anticancer properties. *Biophys. J.* **2006**, *91* (12), 4478–4489.

(20) Keire, D. A.; Kobayashi, M. The orientation and dynamics of substance P in lipid environments. *Protein Sci.* **1998**, *7* (11), 2438–2450.

(21) Sargent, D. F.; Schwyzer, R. Membrane lipid phase as catalyst for peptide−receptor interactions. *Proc. Natl. Acad. Sci. U.S.A.* **1986**, *83* (Aug), 5774–5778.

(22) Schwyzer, R. Membrane-assisted molecular mechanism of neurokinin receptor subtype selection. *EMBO J.* **1987**, *6* (8), 2255–2259.

(23) Schwyzer, R. 100 years lock-and-key concept: Are peptides shaped and guided to their receptors by the target cell membrane. *Biopolymers (Pept. Sci.)* **1995**, *37*, 5–16.

(24) Giragossian, C.; Mierke, D. F. Determination of ligand−receptor interactions of cholecystokinin by nuclear magnetic resonance. *Life Sci.* **2003**, *73* (6), 705–713.

(25) Shacham, S.; Marantz, Y.; Bar-Haim, S.; Kalid, O.; Warshaviak, D.; Avisar, N.; Inbal, B.; Heifetz, A.; Fichman, M.; Topf, M.; Naor, Z.; Noiman, S.; Becker, O. M. PREDICT modeling and in-silico screening for G-protein coupled receptors. *Proteins* **2004**, *57* (1), 51–86.

(26) Cherezov, V.; Rosenbaum, D. M.; Hanson, M. A.; Rasmussen, S. G.; Thian, F. S.; Kobilka, T. S.; Choi, H. J.; Kuhn, P.; Weis, W. I.; Kobilka, B. K.; Stevens, R. C. High-resolution crystal structure of an engineered human beta2-adrenergic G protein-coupled receptor. *Science* **2007**, *318* (5854), 1258–1265.

(27) Rosenbaum, D. M.; Cherezov, V.; Hanson, M. A.; Rasmussen, S. G.; Thian, F. S.; Kobilka, T. S.; Choi, H. J.; Yao, X. J.; Weis, W. I.; Stevens, R. C.; Kobilka, B. K. GPCR engineering yields high-resolution structural insights into beta2-adrenergic receptor function. *Science* **2007**, *318* (5854), 1266–1273.

(28) Kobilka, B. K.; Deupi, X. Conformational complexity of G-protein-coupled receptors. *Trends Pharmacol. Sci.* **2007**, *28* (8), 397–406.

(29) Inooka, H.; Ohtaki, T.; Kitahara, O.; Ikegami, T.; Endo, S.; Kitada, C.; Ogi, K.; Onda, H.; Fujino, M.; Shirakawa, M. Conformation of a peptide ligand bound to its G-protein coupled receptor. *Nat. Struct. Biol.* **2001**, *8* (2), 161–165.

(30) Luca, S.; White, J. F.; Sohal, A. K.; Filippov, D. V.; van Boom, J. H.; Grisshammer, R.; Baldus, M. The conformation of neurotensin bound to its G protein-coupled receptor. *Proc. Natl. Acad. Sci. U.S.A.* **2003**, *100* (19), 10706–10711.

(31) Heise, H.; Luca, S.; de Groot, B. L.; Grubmuller, H.; Baldus, M. Probing conformational disorder in neurotensin by two-dimensional solid-state NMR and comparison to molecular dynamics simulations. *Biophys. J.* **2005**, *89* (3), 2113–2120.

(32) Dong, M.; Ding, X. Q.; Thomas, S. E.; Gao, F.; Lam, P. C.; Abagyan, R.; Miller, L. J. Role of lysine187 within the second extracellular loop of the type A cholecystokinin receptor in agonist-induced activation. Use of complementary charge-reversal mutagenesis to define a functionally important interdomain interaction. *Biochemistry* **2007**, *46* (15), 4522–4531.

(33) Archer-Lahlou, E.; Tikhonova, I.; Escrieut, C.; Dufresne, M.; Seva, C.; Pradayrol, L.; Moroder, L.; Maigret, B.; Fourmy, D. Modeled structure of a G-protein-coupled receptor: the cholecystokinin-1 receptor. *J. Med. Chem.* **2005**, *48* (1), 180–191.

(34) Archer-Lahlou, E.; Escrieut, C.; Clerc, P.; Martinez, J.; Moroder, L.; Logsdon, C.; Kopin, A.; Seva, C.; Dufresne, M.; Pradayrol, L.; Maigret, B.; Fourmy, D. Molecular mechanism underlying partial and full agonism mediated by the human cholecystokinin-1 receptor. *J. Biol. Chem.* **2005**, *280* (11), 10664–10674.

(35) Wuthrich, K. *NMR of Proteins and Nucleic Acids*; John Wiley and Sons: New York, 1986.

(36) Braunschweiler, L.; Ernst, R. R. Coherence transfer by isotropic mixing: application to proton correlation spectroscopy. *J. Magn. Reson.* **1983**, *53*, 521–528.

(37) Jeener, J.; Meier, B. H.; Bachmann, P.; Ernst, R. R. Investigation of exchange processes by two-dimensional NMR spectroscopy. *J. Magn. Reson.* **1979**, *71*, 4546.
(38) Bothner-By, A. A.; Stephens, R. L.; Lee, J.-M.; Warren, C. D.; Jeanloz, R. W. Structure determination of a tetrasacchride: transient nuclear Overhauser effects in the rotating frame. *J. Am. Chem. Soc.* **1984**, *106*, 811–813.
(39) Piotto, M.; Saudek, V.; Sklenar, V. Gradient-tailored excitation for single-quantum NMR spectroscopy of aqueous solutions. *J Biomol NMR* **1992**, *2* (6), 661–665.
(40) Sklenar, V. Suppression of radiation damping in multidimensional NMR experiments using magnetic field gradients. *J. Magn. Reson.* **1995**, *A114*, 132–135.
(41) Sklenar, V.; Piotto, M.; Leppik, R.; Saudek, V. Gradient tailored water suppression for $^{1}H-^{15}N$ HSQC experiments optimized to retain full sensitivity. *J. Magn. Reson., Ser. A* **1993**, *102*, 241–245.
(42) Marion, D.; Wuthrich, K. Application of phase sensitive two-dimensional correlated spectroscopy (COSY) for measurements of 1H−1H spin−spin coupling constants in proteins. *Biochem. Biophys. Res. Commun.* **1983**, *113* (3), 967–974.
(43) States, D. J.; Haberkorn, R. A.; Ruben, D. J. A two-dimensional nuclear Overhauser experiment with pure absorption phase in four quadrants. *J. Magn. Reson.* **1982**, *48*, 286.
(44) Hwang, T.; Shaka, A. Water suppression that works. excitation sculpting using arbitrary wave-forms and pulsed-field gradients. *J. Magn. Reson., Ser. A* **1995**, *112*, 275–279.
(45) Shaka, A.; Lee, C.; Pines, A. Iterative schemes for bilinear operators: application to spin decoupling. *J. Magn. Reson.* **1988**, *77* (2), 274–293.
(46) Brunger, A. T. *X-PLOR: Version 3.1: A System for X-ray Crystallography and NMR*.Yale Unviersity Press: New Haven, CT, 1992.
(47) Wuthrich, K.; Billeter, M.; Braun, W. Pseudo-structures for the 20 common amino acids for use in studies of protein conformations by measurement of intramolecular proton−proton distance constraints with nuclear magnetic resonance. *J. Mol. Biol.* **1983**, *169*, 949–961.
(48) Nigles, M.; Clore, G. M.; Gronenborn, A. M. Determination of three-dimensional structures of proteins from the interproton distance data by hybrid distance geometry-dynamical simulated annealing calculations. *FEBS Lett.* **1988**, *2*, 317–324.
(49) Perczel, A.; Hollosi, M. Turns. In *Circular Dichroism and the Conformational Analysis of Biomolecules*; Fasman, G. Ed.; Plenum Press:New York, 1996; pp 285−380.
(50) Woody, R. W. Contributions of tryptophan side chains to the far-ultraviolet circular dichroism of proteins. *Eur. Biophys. J.* **1994**, *23* (4), 253–262.
(51) Rozek, A.; Friedrich, C. L.; Hancock, R. E. Structure of the bovine antimicrobial peptide indolicidin bound to dodecylphosphocholine and sodium dodecyl sulfate micelles. *Biochemistry* **2000**, *39* (51), 15765–15774.
(52) Ladokhin, A. S.; Selsted, M. E.; White, S. H. CD spectra of indolicidin antimicrobial peptides suggest turns, not polyproline helix. *Biochemistry* **1999**, *38* (38), 12313–12319.
(53) Keire, D. A.; Solomon, T. E.; Reeve, J. R., Jr. NMR evidence for different conformations of the bioactive region of rat CCK-8 and CCK-58. *Biochem. Biophys. Res. Commun.* **2002**, *293* (3), 1014–1020.
(54) Keire, D. A.; Solomon, T. E.; Reeve, J. R., Jr. Identical primary sequence but different conformations of the bioactive regions of canine CCK-8 and CCK-58. *Biochem. Biophys. Res. Commun.* **1999**, *266* (2), 400–404.
(55) Wishart, D. S.; Bigam, C. G.; Yao, J.; Abildgaard, F.; Dyson, H. J.; Oldfield, E.; Markley, J. L.; Sykes, B. D. $^{1}H^{13}C^{15}N$ chemical shift referencing in biomolecular NMR. *J. Biomol. NMR* **1995**, *6*, 135–140.
(56) Wishart, D. S.; Bigam, C. G.; Holm, A.; Hodges, R. S.; Sykes, B. D. $^{1}H^{13}C^{15}N$ random coil NMR chemical shifts of the common amino acids. I. Investigations of nearest-neighbor effects. *J. Biomol. NMR* **1995**, *5* (1), 67–81.
(57) Laskowski, R. A.; Rullmannn, J. A.; MacArthur, M. W.; Kaptein, R.; Thornton, J. M. AQUA and PROCHECK-NMR: programs for checking the quality of protein structures solved by NMR. *J. Biomol. NMR* **1996**, *8* (4), 477–486.
(58) Clore, G. M.; Robien, M. A.; Gronenborn, A. M. Exploring the limits of precision and accuracy of protein structures determined by nuclear magnetic resonance spectroscopy. *J. Mol. Biol.* **1993**, *231* (1), 82–102.
(59) Whitehead, T. L.; McNair, S. D.; Hadden, C. E.; Young, J. K.; Hicks, R. P. Membrane-induced secondary structures of neuropeptides: a comparison of the solution conformations adopted by agonists and antagonists of the mammalian tachykinin NK1 receptor. *J. Med. Chem.* **1998**, *41* (9), 1497–1506.
(60) Keire, D. A.; Fletcher, T. G. The conformation of substance P in lipid environments. *Biophys. J.* **1996**, *70* (4), 1716–1727.
(61) Lee, A. G. How lipids affect the activities of integral membrane proteins. *Biochim. Biophys. Acta* **2004**, *1666* (1−2), 62–87.
(62) Pucadyil, T. J.; Kalipatnapu, S.; Harikumar, K. G.; Rangaraj, N.; Karnik, S. S.; Chattopadhyay, A. G-protein-dependent cell surface dynamics of the human serotonin1A receptor tagged to yellow fluorescent protein. *Biochemistry* **2004**, *43* (50), 15852–15862.
(63) Harikumar, K. G.; Puri, V.; Singh, R. D.; Hanada, K.; Pagano, R. E.; Miller, L. J. Differential effects of modification of membrane cholesterol and sphingolipids on the conformation, function, and trafficking of the G protein-coupled cholecystokinin receptor. *J. Biol. Chem.* **2005**, *280* (3), 2176–2185.
(64) Paila, Y. D.; Pucadyil, T. J.; Chattopadhyay, A. The cholesterol-complexing agent digitonin modulates ligand binding of the bovine hippocampal serotonin 1A receptor. *Mol. Membr. Biol.* **2005**, *22* (3), 241–249.
(65) Chachisvilis, M.; Zhang, Y. L.; Frangos, J. A. G protein-coupled receptors sense fluid shear stress in endothelial cells. *Proc. Natl. Acad. Sci. U.S.A.* **2006**, *103* (42), 15463–15468.
(66) Raghuraman, H.; Chattopadhyay, A. Melittin: A Membrane-active Peptide with Diverse Functions. *Biosci. Rep.* **2006**, *27*, 189–223.
(67) Romano, R.; Musiol, H. J.; Weyher, E.; Dufresne, M.; Moroder, L. Peptide hormone−membrane interactions: the aggregational and conformational state of lipogastrin derivatives and their receptor binding affinity. *Biopolymers* **1992**, *32* (11), 1545–1558.
(68) Romano, R.; Dufrense, M.; Prost, M. C.; Bali, J. P.; Bayerl, T. M.; Moroder, L. Peptide hormone−membrane interactions. Intravesicular transfer of lipophilic gastrin derivatives to artificial membranes and their bioactivities. *Biochim. Biophys. Acta* **1993**, *1145*, 235–242.
(69) Lutz, J.; Romano-Gotsch, R.; Escrieut, C.; Fourmy, D.; Matha, B.; Muller, G.; Kessler, H.; Moroder, L. Mapping of ligand binding sites of the cholecystokinin-B/gastrin receptor with lipogastrin peptides and molecular modeling. *Biopolymers* **1997**, *41* (7), 799–817.
(70) Moroder, L. On the mechanism of hormone recognition and binding by the CCK-B/gastrin receptor. *J. Pept. Sci.* **1997**, *3* (1), 1–14.
(71) Moroder, L.; Romano, R.; Guba, W.; Mierke, D. F.; Kessler, H.; Delporte, C.; Winand, J.; Christophe, J. New evidence for a membrane-bound pathway in hormone receptor binding. *Biochemistry* **1993**, *32* (49), 13551–13559.
(72) Giragossian, C.; Mierke, D. F. Intermolecular interactions between cholecystokinin-8 and the third extracellular loop of the cholecystokinin-2 receptor. *Biochemistry* **2002**, *41* (14), 4560–4566.
(73) Giragossian, C.; Pellegrini, M.; Mierke, D. F. NMR studies of CCK-8/CCK1 complex support membrane-associated pathway for ligand-receptor interaction. *Can. J. Physiol. Pharmacol.* **2002**, *80* (5), 383–387.
(74) Giragossian, C.; Stone, S.; Papini, A. M.; Moroder, L.; Mierke, D. F. Conformational and molecular modeling studies of sulfated cholecystokinin-15. *Biochem. Biophys. Res. Commun.* **2002**, *293* (3), 1053–1059.
(75) Albrizio, S.; Carotenuto, A.; Fattorusso, C.; Moroder, L.; Picone, D.; Temussi, P. A.; D'Ursi, A. Environmental mimic of receptor interaction: conformational analysis of CCK-15 in solution. *J. Med. Chem.* **2002**, *45* (4), 762–769.
(76) Jacobs, R. E.; White, S. H. The nature of the hydrophobic binding of small peptides at the bilayer interface: implications for the insertion of transbilayer helicies. *Biochemistry* **1989**, *28*, 3421–3437.
(77) Wishart, D. S.; Sykes, B. D.; Richards, F. M. The chemical shift index: a fast and simple method for the assignment of protein secondary structure through NMR spectroscopy. *Biochemistry* **1992**, *31* (6), 1647–1651.
(78) de Planque, M. R.; Bonev, B. B.; Demmers, J. A.; Greathouse, D. V.;.; Koeppe, R. E., 2nd; Separovic, F.; Watts, A.; Killian, J. A. Interfacial anchor properties of tryptophan residues in transmembrane peptides can dominate over hydrophobic matching effects in peptide−lipid interactions. *Biochemistry* **2003**, *42* (18), 5341–5348.
(79) Fournie-Zaluski, M. C.; Durieux, C.; Lux, B.; Belleney, J.; Pham, P.; Gerard, D.; Roques, B. P. Conformational analysis of cholecystokinin fragments CCK4, CCK5, and CCK6 by 1H-NMR spectroscopy and fluorescence-transfer measurements. *Biopolymers* **1985**, *24*, 1663–1681.
(80) Loomis, R. E.; Lee, P. C.; Tseng, C. C. Conformational analysis of the cholecystokinin C-terminal octapeptide: a nuclear magnetic resonance and computer-simulation approach. *Biochim. Biophys. Acta* **1987**, *911* (2), 168–179.
(81) Moroder, L.; D'Ursi, A.; Picone, D.; Amodeo, P.; Temussi, P. A. Solution conformation of CCK9, a cholecystokinin analog. *Biochem. Biophys. Res. Commun.* **1993**, *190* (3), 741–746.

JM701401J